Available online at www.sciencedirect.com

ScienceDirect

Nuclear Physics A 967 (2017) 696–699

NUCLEAR PHYSICS A

www.elsevier.com/locate/nuclphysa

Direct photon measurements in pp and Pb-Pb collisions with the ALICE experiment

M. Germain,
on behalf of the ALICE Collaboration

SUBATECH, IMT-Atlantique, Université de Nantes, CNRS-IN2P3, Nantes, France

Abstract

Direct photon production in heavy-ion collisions provides a valuable set of observables to study the hot QCD medium. The direct photons are produced at different stages of the collision and escape the medium unaffected. In heavy-ion collisions, the direct photon yield at high transverse momentum (p_{T}> 5 GeV/c) is dominated by prompt photons produced in hard scattering of incoming partons and provides information on nuclear parton distribution functions and on the initial parton dynamics. The low momentum component ($p_{\mathrm{T}} \lesssim$ 5 GeV/c) of the direct photon production is dominated by thermal radiation by the hot and dense matter created, carrying information on its space-time evolution, collective flow and temperature.

We present recent ALICE results on direct photon production Pb-Pb collisions at 2.76 TeV and on direct photon production in pp at 7 TeV using isolation techniques. The results are compared to theoretical predictions and previous measurements.

Keywords: photons, direct photons, QGP, electromagnetic probes, heavy-ions, pQCD, NLO

1. Introduction

The production of direct photons, defined as photons not originating from hadron decays, in pp collisions, allows a test of perturbative QCD (pQCD) predictions [1] and constrains the proton parton distribution functions (PDF) [2]. At high p_{T} and Leading Order (LO) pQCD, the following processes contribute to the direct photon production: the quark-gluon Compton scattering, which is dominant and allows probing the gluon PDF, the quark-antiquark annihilation, and the fragmentation of a final state parton into a photon. In this latter process the connection with hard scattering dynamic is partly lost, but isolation techniques helps in reducing such contribution [2]. In nucleus-nucleus collisions direct photons are produced at all stages of the collision: by the initial hard processes described before, but also by the thermal radiation of the deconfined quark-gluon matter as well as hadronic matter created in the collision. The thermal photons, typically emitted with low transverse momentum ($p_{\mathrm{T}} \lesssim$5 GeV/c) carry information on the temperature, collective flow, and space-time evolution of the hot medium [3].

http://dx.doi.org/10.1016/j.nuclphysa.2017.05.094
0375-9474/© 2017 The Author(s). Published by Elsevier B.V.
This is an open access article under the CC BY license (http://creativecommons.org/licenses/by/4.0/).

2. Direct photons at low and intermediate p_{T} in pp and Pb-Pb collisions: R_γ

In the analysis presented here, the inclusive yield of photons is measured via two independent methods: with the PHOton Spectrometer (PHOS), a highly segmented electromagnetic calorimeter, and via Photon Conversion Method (PCM) by reconstructing secondary vertices of the e^+e^- pairs from photons converted in the inner material of ALICE. The details of this measurement have been published in [4]. The PHOS calorimeter measures the electromagnetic shower left by photons via the scintillation light generated in the segmented (2×2 cm^2) $PbWO_4$ crystals. Its coverage is $260^{\mathrm{o}} < \varphi < 320^{\mathrm{o}}$ and $|\Delta\eta| < 0.13$ [5]. The photons are selected using a combination of cuts on energy, size and dispersion of the shower. In the PCM analysis, the large acceptance (2π in φ, $|\Delta\eta| < 0.9$) of the central barrel detectors, the Inner Tracking System (ITS) and the Time Projection Chamber (TPC), allows a compensation of the low conversion probability of $\simeq 8.5\%$. The photon sample is then obtained by applying dedicated cuts on the decay topology and on electron track properties. The Pb-Pb analysis at $\sqrt{s_{NN}} = 2.76$ TeV is performed in three centrality bins (0-20%, 20-40% and 40-80%). The direct photon signal is obtained statistically by subtracting from the inclusive photon yield the decay photon component by using the double ratio R_γ method [6]. The decay photon component is dominated by π^0 and η and is derived from the measured π^0 spectrum using m_{T} scaling for η, η', ω, ϕ and ρ^0. Finally the direct yield is obtained from the the inclusive spectra $\gamma_{direct} = \gamma_{incl} - \gamma_{decay} = (1 - \frac{1}{R_\gamma}).\gamma_{incl}$ where the use of the double ratio $R_\gamma = \frac{\gamma_{incl}}{\gamma_{decay}} \equiv \frac{\gamma_{incl}}{\pi^0_{param}} / \frac{\gamma_{decay}}{\pi^0_{param}}$ (where π^0_{param} is the parametrisation of the measured π^0 spectrum) reduces the systematic uncertainties, since the measured π^0 and γ_{incl} spectrum share some of the systematic errors. The results for R_γ obtained in pp at 7 TeV at low p_{T} were compatible with unity, indicating no direct photon excess [7] whereas the values in Pb-Pb collisions at $\sqrt{s_{NN}} = 2.76$ TeV are presented in Fig. 1 [4]. The measurements are also compared to prompt photon expectations calculated with next-to-leading-order (NLO) pQCD calculations [8, 9, 10]. In all centrality classes R_γ agrees with the calculations above $p_{\mathrm{T}} \gtrsim 5$ GeV/c. For the most central collisions, an excess in data below $p_{\mathrm{T}} \lesssim 2$ GeV/c is observed which indicates an additional source of direct photons in central collisions.

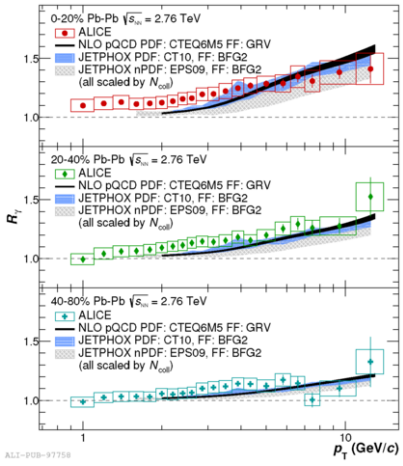

Fig. 1. Combined PCM and PHOS double ratio R_γ for three centrality classes compared to NLO pQCD calculations for nucleus-nucleus collisions scaled by the number of binary collisions for each centrality classes [4].

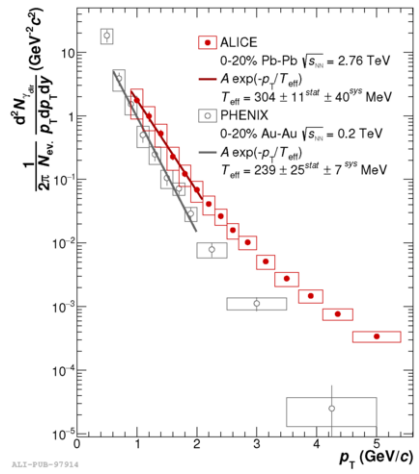

Fig. 2. Direct photon spectrum for the 0-20% most central events in Pb-Pb collisions at $\sqrt{s_{NN}} = 2.76$ TeV [4] and in Au+Au at $\sqrt{s_{NN}}$=200 GeV/c [11].

The direct photon spectrum for the most central (0-20%) Pb-Pb collisions is presented in Fig. 2 and compared to the results obtained at RHIC [11]. An exponential fit is shown for both spectra at low p_{T} ($1 < p_{\mathrm{T}} < 2$ GeV/c) which enables to extract the slope parameters. The value obtained by ALICE in central collisions for the slope parameter is $T_{\mathrm{eff}} = 304 \pm 11^{\mathrm{stat}} \pm 40^{\mathrm{syst}}$ MeV, higher than in PHENIX. The relation between the inverse slope parameter and the initial temperature is not direct due to contribution of blueshifted

photons from the late stages of the collision but this results is consistent with a larger initial temperature of the medium for higher collision energy and/or with a higher boost velocity at the LHC.

3. Direct photons at high p_{T} in pp collisions: Isolation technique

The analysis of direct photons at high p_{T} has been performed on pp collisions at $\sqrt{s} = 7$ TeV, using data collected in 2011. In this analysis, the photons are measured in the ALICE Electromagnetic Calorimeter (EMCal). The EMCal [12] is a lead-scintillator sampling calorimeter consisting of cells of $\Delta\eta \times \Delta\varphi = 0.0143 \times 0.0143$ size with a coverage of $1.4 < \varphi < \pi$, $|\Delta\eta| \leq 0.7$. In order to collect a high-p_{T} sample we took data with the L0-EMCal trigger based on the analog charge sum of 2× 2 cells, in correlation with the Minimum Bias (MB) trigger signal in the two V0 detectors placed at large rapidities ($2.8 < \eta < 5.1, -3.7 < \eta < -1.7$). The clusters in EMCal are reconstructed by aggregating cells with energy deposit $E_{cell} \geq 100$ MeV to a leading cell with at least $E_{\mathrm{seed}} \geq 300$ MeV. The rejection of clusters from charged particles is based on proximity cuts between charged tracks, measured in the central detectors extrapolated to the EMCAL surface, and EMCAL clusters. The main source of background of direct photons consists of neutral mesons 2-γ decays especially from π^o. The showers from the two decay photons merge in one single cluster in the range $10 < p_{\mathrm{T}} < 60$ GeV/c, resulting in elongated clusters. The elongation of clusters can be measured with the largest eigenvalue of the cluster's energy decomposition in the EMCal $\eta - \varphi$ plane σ^2_{long} , $\sigma^2_{\mathrm{long}} = 0.5\left(\sigma^2_{\varphi\varphi} + \sigma^2_{\eta\eta} + \sqrt{(\sigma_{\varphi\varphi} - \sigma_{\eta\eta})^2 + 4\sigma^2_{\eta\varphi}}\right)$ where the dispersions σ^2_{ij} are computed with a logarithmic weight [13]. The photon selection is based on a cut on the cluster elongation σ^2_{long}. In order also to decrease the contamination of photons produced in fragmentation processes (including decay photons), we use isolation techniques [2]. The isolation method relies on the measurement of the total energy $E_{\mathrm{T}}^{\mathrm{ISO}}$ in a cone of radius $R = \sqrt{\Delta\varphi^2 + \Delta\eta^2} = 0.4$ around the photon candidate, including both the charged contribution, from tracks reconstructed by the ALICE central barrel and the electromagnetic contribution, from EMCal neutral clusters. The isolation criterion is then $E_{\mathrm{T}}^{\mathrm{ISO}} < 2$ GeV/c. An additional cut in photon candidate acceptance is applied to impose the isolation cone to be contained in EMCAL acceptance, reducing the measurement to $1.8 < \varphi < 2.7$, $|\Delta\eta| \leq 0.27$. A non negligible residual contamination of background candidates is expected in the isolated photon sample. Its estimation is performed through a double side-band counting method in the $E_{\mathrm{T}}^{\mathrm{ISO}}$, σ^2_{long} plane. The method assumes that the $E_{\mathrm{T}}^{\mathrm{ISO}}$ is independent of the shower elongation in the background region and the signal contamination is small in the background regions. These hypotheses have been studied in Monte Carlo samples of signal and background and a correction has been extracted to take into account the effect of the $E_{\mathrm{T}}^{\mathrm{ISO}}$- σ^2_{long} correlation and of leakage of signal in background region. This leads to a purity of the isolated photon sample going from 28% to 80% with increasing energy. The isolated photon spectrum is then corrected by the reconstruction and identification and isolation efficiency. Finally the differential cross section is obtained by scaling the isolated photon spectrum by the trigger efficiency and the MB trigger cross section measured in ALICE [14].

The systematic uncertainties on the measurement are estimated by varying the different cuts used in the analysis. The overall systematic uncertainty was found to be between 13 and 20%, the main source being the discrepancy between the modeling of the shower shape in simulations compared to the data. Further investigations on this discrepancy are ongoing in order to reduce its contribution to the systematic uncertainty on the contamination. The isolated photon cross section is shown on Fig. 3. The ALICE measurement allows reaching lower E_{T} than the previous LHC measurements by ATLAS ($E_{\mathrm{T}} > 15$ GeV) [16] and CMS ($E_{\mathrm{T}} > 30$ GeV) [17]. The results are also compared to the JETPHOX predictions [15] in Fig. 3 and Fig. 4, which indicates a good agreement with NLO pQCD predictions over the whole E_{T} range.

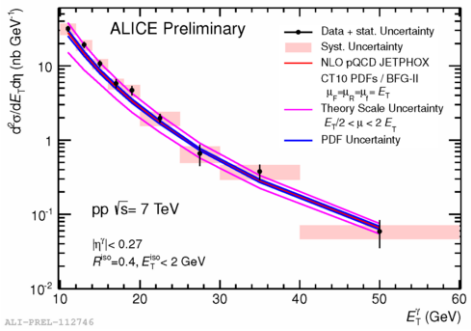

Fig. 3. Differential isolated photon cross section as a function of the photon transverse energy in pp collisions at $\sqrt{s}$ = 7 TeV measured in ALICE.

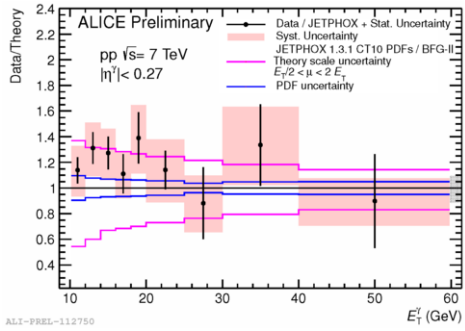

Fig. 4. Comparison of the isolated photon cross section in pp collisions at $\sqrt{s}$ = 7 TeV measured in ALICE with a NLO pQCD calculation [15] .

4. Summary

The measurement of direct photons in ALICE in pp and Pb-Pb collisions is presented. At low p_T the measurement is performed via statistical method using two different analyses, in the calorimeter (PHOS) and in the central barrel with Photon Conversion Method. The measurement in Pb-Pb in three centrality classes shows a clear direct photon signal in the double ratio (R_γ) and an excess with respect to NLO prediction is found in the most central collisions. The effective temperature of the medium is estimated to $T_{\rm eff}$ = 304 $\pm 11^{\rm stat} \pm 40^{\rm syst}$ MeV from a fit of the direct photon spectrum [4]. In pp collisions, at low p_T no excess was found. At high p_T , the direct isolated photon cross section is measured by using the the EMCal calorimeter. The results allow the extension the measurement to lower p_T compared to the other LHC experiments. The results agree with NLO calculation for the whole measured p_T range.

References

[1] P. Aurenche, R. Baier, M. Fontannaz, D. Schiff, Nucl. Phys. B 297 (4) (1988) 661 – 696.
[2] R. Ichou, D. d'Enterria, Phys. Rev. D 82 (2010) 014015.
[3] C. Gale, Elementary particles, nuclei and atoms volume 23, copyright 2010 Springer-Verlag Berlin Heidelberg, accessed 2017-04-04.
[4] J. Adam, et al., Phys. Lett. B 754 (2016) 235 – 248.
[5] D. Dellacasa, et al., Alice technical design report of the photon spectrometer (phos). arXiv:CERN-LHC-99-04.
[6] A. Adler, et al., Phys. Rev. Lett. 94 (2005) 232301.
[7] M. Wilde, et al., Nucl. Phys. A904-905 (2013) 573c–576c.
[8] M. Klasen, C. Klein-Bösing, F. König, J. Wessels, JHEP (10) (2013) 119.
[9] W. Vogelsang, M. R. Whalley, Journal of Phys. G: 23 (7A) (1997) A1.
[10] L. E. Gordon, W. Vogelsang, Phys. Rev. D48 (1993) 3136–3159.
[11] A. Adare, et al., Phys. Rev. C 91 (2015) 064904.
[12] U. Abeysekara, et al., ALICE EMCal Physics Performance Report (2010). arXiv:1008.0413.
[13] T. Awes, F. Obenshain, F. Plasil, S. Saini, S. Sorensen, G. Young, Nucl. Instr. and Meth. A311 (1) (1992) 130 – 138.
[14] B. Abelev, et al., Eur. Phys. J. C 73 (6) (2013) 2456.
[15] P. Aurenche, M. Fontannaz, J.-P. Guillet, E. Pilon, M. Werlen, Phys. Rev. D73 (2006) 094007.
[16] G. Aad, et al., Phys. Rev. D83 (2011) 052005.
[17] S. Chatrchyan, et al., Phys. Rev. D84 (2011) 052011.